Genome Biology

Reverse-engineering Arabidopsis thaliana transcriptional network under changing environmental conditions

Genome Biology 2009, **10**:R96 doi:10.1186/gb-2009-10-9-r96

Javier Carrera (javier.carrera@synth-bio.org)
Guillermo Rodrigo (guirodta@ibmcp.upv.es)
Alfonso Jaramillo (alfonso.jaramillo@gmail.com)
Santiago F Elena (sfelena@ibmcp.upv.es)

ISSN 1465-6906

Article type Research

Submission date 10 July 2009

Acceptance date 15 September 2009

Publication date 15 September 2009

Article URL http://genomebiology.com/2009/10/9/R96

Reverse-engineering *Arabidopsis thaliana* transcriptional network under changing environmental conditions

Javier Carrera,[1,2*] Guillermo Rodrigo,[1*] Alfonso Jaramillo,[3,4] and Santiago F Elena[1,5]

[*]Authors have contributed equally to this manuscript

For correspondence: Santiago F Elena. sfelena@ibmcp.upv.es

[1] Instituto de Biología Molecular y Celular de Plantas, Consejo Superior de Investigaciones Científicas-UPV, Ingeniero Fausto Elio s/n, 46022 València, Spain

[2] ITACA, Universidad Politécnica de Valencia, Ingeniero Fausto Elio s/n, 46022 València, Spain

[3] Laboratoire de Biochimie, École-Polytechnique-CNRS UMR7654, Route de Saclay, 91128 Palaiseau, France

[4] Epigenomics Project, Genopole-Université d'Évry Val d'Essonne-CNRS UPS3201, 523 Terrasses de l'Agora, 91034 Évry, France

[5] The Santa Fe Institute, 1399 Hyde Park Road, Santa Fe, NM 87501, USA

Abstract

Background

Understanding the molecular mechanisms plants have evolved to adapt their biological activities to a constantly changing environment is an intriguing question and one that requires a systems biology approach. Here we present a network analysis of genome-wide expression data combined with reverse-engineering network modelling to dissect the transcriptional control of *A. thaliana*. The regulatory network is inferred by using an assembly of microarray data containing steady-state RNA expression levels from several growth conditions, developmental stages, biotic and abiotic stresses, and a variety of mutant genotypes.

Results

We show that *A. thaliana* regulatory network has the characteristic properties of hierarchical networks. We successfully applied our quantitative network model to predict the full transcriptome of the plant for a set of microarray experiments not included in the training dataset. We also used our model to analyze the robustness in expression levels conferred by network motifs such as the coherent feedforward loop. In addition, the meta-analysis presented here has allowed us to identify regulatory and robust genetic structures.

Conclusions

These data suggest that *A. thaliana* has evolved a high connectivity in terms of transcriptional regulations among cellular functions involved in response and adaptation to changing environments; while gene networks constitutively expressed or less related to stress response are characterized by a lower connectivity. Taken together, these findings suggest conserved regulatory strategies that have been selected during the evolutionary history of this Eukaryote.

Background

Living organisms have evolved molecular circuitries with the aim of promoting their own development under dynamically changing environments. In particular, plants are not able to evade those changes and have had to evolve robust methods to cope with environmental stress and recovery mechanisms. Genomic sequences specify the context-dependent gene expression programs to render cells, tissues, organs and, finally, organisms. Then, at any moment during cell cycle and at each stage of an organism's development, and in response to environmental conditions, each cell is the product of specific and well defined programs involving the coordinated transcription of thousands of genes. Thus, the elucidation of such programs by means of the regulatory interactions is pivotal for the understanding of how organisms have evolved and what environments may have conditioned evolutionary trajectories the most. However, understanding how this highly tuned process is achieved is still beyond our knowledge for most organisms, and the surface of the problem is only being scratched for a handful of model organisms such as the bacterium *Escherichia coli* [1], the yeast *Saccharomyces cerevisiae* [2], the nematode *Caenorhabditis elegans* [3], the plant *Arabidopsis thaliana* [4,5], or to a lesser extent for humans [6].

Meta-analyses of microarray data collections may now be used to construct biological networks that systematically categorize all molecules and describe their functions and interactions. Networks can integrate biological functions of cells, organs, and organisms. During recent years, there has been a tremendous effort in the development and improvement of techniques to infer gene connectivity. Clustering approaches [7-11] and information theory methods [12-16] have been used to infer regulatory networks. Bayesian methods [17-20] can give accurate networks with low coverage but at a high computational cost.

The analysis of the expression of *A. thaliana* transcriptome offers the potential to identify prevailing cellular processes, to associate genes with particular biological functions, and to assign otherwise unknown genes to biological responses to which they are correlated. Previous attempts to model *A. thaliana* gene network used methods such as fuzzy *k*-means clustering [21], graphical Gaussian models [4], and Markov chain graph clustering [5,15]. The inconvenience of the first approach is that clustering describes genes based on a characteristic property common to all genes but it is difficult to deduce a pathway structure from this property alone, because pathways would have to be concerned with co-expression features that transcend such cluster structure. The second approach assumes that the number of microarray slides should be much larger than the number of genes analyzed or approximations must be taken (e.g. empirical Bayes with bootstrap resampling or shrinkage approaches). The last approach is still based on Person's correlations and therefore, strongly sensitive to outliers and to violations to the implicit assumption of linear relationships among genes. In this article, we present a predictable genome model from a regulatory scaffold inferred by using probabilistic methods [15] and estimate the corresponding kinetic parameters using linear regression [22-25]. We analyze the topological properties and predictive power of the inferred regulatory model. We evaluate the performance of the network by predicting already known transcriptional regulations and assess the functional relevance and reproducibility of the co-expression patterns detected. Finally, we discuss the evolutionary implications of the transcriptional control in plants.

Results

High-throughput technologies combined with rigorous and biologically-rooted modeling will allow understanding how simple genetic or environmental perturbations influence the dynamic behavior of cellular genetic and metabolic networks [26]. However, transcriptomic data need to be properly integrated to formulate a model that can be used for making quantitative predictions on how the environment interacts with cellular networks to affect phenotypic responses. At the end, the accurate prediction of this quantitative behavior will open the possibility of re-engineering cellular circuits. To reach this end, we have attempted the integration of experimental and computational approaches to construct a predictive gene regulatory network model covering the full transcriptome of the model plant *A. thaliana*.

Genome-wide transcriptional control in *A. thaliana*

In the present work, we have applied a recently developed inference methodology, *InferGene* [25], to obtain a gene regulatory model, suitable for analyzing optimality and allowing studying the transcriptional control response under changing environments in *A. thaliana*. For that, we have considered the Affymetrix's chip for the *A. thaliana* genome, from which we selected 22,094 non-redundant genes, of which about 1187 are putative transcription factors (TFs) (see Material and Methods). The data used for the inference procedure were a compendium of 1436 Affymetrix's microarray hybridization experiments publicly available at the TAIR website and that were normalized using RMA [27]. Here we used the whole expression set (1436 experiments) to construct the model. In Figure 1 we show the inferred transcriptional regulatory network of *A. thaliana* drawn using the Cytoscape viewer [28]; Table 1 collates some parameters describing the topology of the network.

Three types of efficiencies, precision (*P*), sensitivity (*S*) and absolute efficiency (*F*), have been computed to assess the ability of the above inferred network to predict the 448 experimentally validated transcriptional regulations collected in the *AtRegNet* database. *P* is the fraction of predicted interactions that are correct $P = TP/(TP + FP)$ and *S* the fraction of all known interactions that are discovered by the model $S = TP/(TP + FN)$, where *TP* is the number of true positives, *FN* the number of false negatives and *FP* the number of false positives. *F* thus represents the absolute efficiency and it is computed as $F = 2PS/(P + S)$ which is the harmonic mean of precision and sensitivity. Indeed, precision and sensitivity are necessarily negatively correlated performance statistics, and these two values were set up so they maximize global performance (*F*) by selecting values > 5 (Figures S1 and S2 in Additional data file 1) for the *z*-score used as threshold to predict the transcriptional regulations. Figure S3 in Additional data file 1 shows *P*, *S* and *F* as a function of the *z*-score threshold. Sensitivity is maximized $S = 100\%$ for $z = 0$ (i.e., high number of regulations but very low confidence) while precision is maximized $P = 100\%$ for $z = 11$ (i.e., high confidence but very low number of regulations). The optimum value is reached for $z = 5$, a value for which $F = 26\%$ ($P = 40\%$ and $S = 20\%$). In a recent study, a smaller network topology has been proposed for *A. thaliana* [4]. This network contains 18,625 regulations and an $F = 3.7\%$ ($P = 88\%$ but $S = 1.8\%$), relative to the *AtRegNet* reference dataset.

InferGene predicts that more than half of the genes are controlled by constitutive promoters (17.89%) or by promoters regulated by less than three TFs (Table 1). Also, from a purely topological perspective, the inferred transcriptional network of *A. thaliana* is weakly connected directed, containing 18,169 genes connected (see Table 1), while the size of the largest strongly connected component only contains 730 nodes, all

of which are TFs. In addition, it has a high density (0.078%; Table 1), understanding this parameter as the normalized average connectivity of a gene in the network, in comparison to values reported in similar studies done for other organisms. For example, Lee *et al*. [2] suggested a network density of 0.0027% for *S. cerevisiae*, while we previously reported a value of 0.036% for the network inferred for *E. coli* [25]. The characteristic path length [29] of the network follows a Gaussian distribution with an average value of 5.065 edges (Table 1 and Figure S4 in Additional data file 1) and, specifically, the distance between two genes for which a path exists ranges from 1 to 13 edges. In a previous study, we estimated that the characteristic path length for *E. coli* network was 1 [25], much smaller than for the case of *A. thaliana*. Furthermore, the *E. coli* inferred network, did not contain any strongly connected components and its largest weakly directed subnetwork only contained 4 TFs. Other relevant statistical properties of networks are the stress distribution (Figure S5 in Additional data file 1), i.e., the number of paths in which a gene is involved, and the betweenness centrality distribution (Figure 2d), i.e., the number of shortest pathways in which a particular gene is involved. Both distributions are highly asymmetrical, with many nodes having a low betweenness centrality and a few cases with high values (Figure 2d) and with the number of shortest paths per gene smoothly increasing until reaching a maximum of approximately 10^5 short paths per gene and then followed by a drastic drop, with very few genes (around 5) having 10^7 short paths (Figure S5 in Additional data file 1). Ten genes (*At1g32330*, *At4g26930*, *At1g24110*, *At4g24490*, *At2g36590*, *At1g01030*, *At1g76900*, *At2g19050*, *At2g03840*, and *At3g19870*) are connected among them but remain isolated from the rest of the main network (Figure 1), the number of shortest paths for these genes ranges from 1 to 3 (Figure S5 in Additional data file 1). All these genes but the last one are involved in several and apparently loosely related GO functional

categories that include regulation of transcription, transportation and signal transduction, and development and senescence.

Next, we sought to explore whether the inferred regulatory network has scale-free properties. It has been suggested that the distribution of outcoming connections should belong to the class of scale-free small-world networks, representing the potential of transcription factors to regulate multiple target genes whereas the distribution of incoming connectivities would be more exponential-like because the regulation by multiple TFs should be less common that the regulation of several targets by a given TF [30]. Figure 2a shows the distribution of outgoing connectivities per TF, whereas Figure 2b shows the same distribution but only for incoming connectivities per gene. As expected, the outcoming connectivity is best fitted by a truncated power-law (i.e., the Weibull distribution) with exponent $\gamma = 0.902$ and cut-off $k_c = 99.093$ (Table S1 in Additional file 2; $R^2 = 0.949$; Akaike's weight over a set of 10 competing models > 99.99%). This distribution indicates that outcoming connectivities has a scale-free behavior in the range $1 \leq k < k_c$ but deviates from this for connectivities over the cut off. According to Barabási & Oltvai [31], scale free properties arise when hub genes are related in a hierarchical way, with the hub receiving most links being connected to a small fraction of all nodes. In the case of incoming connectivities, the model that better describes the data is a restricted exponential, the half-Normal distribution (Table S1 in Additional file 2; $R^2 = 0.983$; Akaike's weight > 99.99%). Taken together, these two observations suggest that *A. thaliana* transcriptional network contains a few highly connected regulators (Table 2) that play a central role in mediating interactions among a large number of less connected genes. Notice that there are 88.4% TFs regulating more than 10 genes, 36.3% regulating more than 100 genes and just 2.6% that control over 500 genes. For the sake of comparison, it is worth mentioning that in the case of *S.*

cerevisiae the critical exponents estimated for the outcoming connectivity distribution (γ = 0.96 [2,32]) is quite similar to the one here reported. However, the estimate obtained for *E. coli* was smaller (γ = 0.87), a result that suggests that hubs are more important in bacteria than in the two eukaryotes [31]. We have validated the set of predicted targets for the 25% most highly connected TFs using *AtRegNet*, recovering 80% of known interactions for the regulatory model and up to 85% for the effective model (i.e., the one containing both gene-to-gene and gene-to-TF interactions). Figure 2c shows that the scaling of the average clustering coefficient with the number of genes with *k*-connections is approximately lineal in a log-log scale in the range (1 – 10000) of neighbors with slope –1.05 (R^2 = 0.850). Barabási & Oltvai [31] and Ravasz & Barabási [33] have suggested that whenever clustering scales with the number of nodes with slope –1, as it is our case, it has to be taken as a strong indication of hierarchical modularity, i.e. genes cluster in higher-order units of different modularity, a finding that has been suggested as general for system-level cellular organization in plants [34]. Similarly, when the effective model is analyzed, it shows similar results than for the regulatory model. The outcoming connectivities per gene follows a truncated power law with scale-free behavior up to k_c = 21.341 connections per gene and with an exponent γ = 0.765 (Table S1 in Additional file 2; R^2 = 0.998, Akaike's weight > 99.99%) (Figure 2e). Figure 2f shows that the incoming connectivity per gene does not present scale-free properties as it fits to a Normal distribution (Table S1 in Additional file 2; R^2 = 0.998, Akaike's weight > 99.99%).

The environment significantly influences the dynamic expression and assembly of all components encoded in the *A. thaliana* genome into functional biological subnetworks. We have computed the clustering coefficient for all subnetworks with the largest normalized index of connectivity between genes involved in the subnetwork. The

subnetworks were then ranked according to these numbers and the top 12 networks are shown in Table 3. Interestingly, four of these highly connected subnetworks are involved in response to external influences as, for example response to pathogens and other processes related with abiotic stresses (heat, salinity, light, redox). For the sake of illustration, Figure 3 shows the inferred subnetworks for three abiotic and three biotic responses. Particularly, we have made a comprehensive analysis for the subnetwork of the Systemic Acquired Resistance (Figure 3d) and found that the fraction of predicted interactions is $P = 33\%$. Not surprisingly, all genes involved in that subnetwork appear associated with GO categories related to response to stress, like defense to pathogens, response to other organisms such as fungus, bacterium and insects, and response to cold.

Transcriptomic profile prediction

The basic premise of our approach was to use transcriptomic data from multiple perturbation experiments (either genetic or environmental) and quantitatively measure steady-state RNA concentrations to assimilate these expression profiles into a network model that can recapitulate all observations. Now, we develop a second model (test model) excluding the 10% of experiments to quantify the prediction power. The data set was randomly split into two subsets. The first larger subset contained 1292 experiments and was used as training set for inferring a transcription network containing 128,422 regulatory interactions. The second, smaller, subset contained 144 array experiments and was used for validation purposes.

As a first measure of the performance of our test model network in predicting responses to stresses, we have used it along with the expression levels of all the TFs for each experimental condition, c, to predict global expression profiles. Then, the

predicted expression values for each of the 22,094 individual genes included in the Affymetrix array, $\hat{y}_{gc}$, were compared with the corresponding empirical measurements, y_{gc}, using the deviation statistic $\Delta_g = \frac{1}{N_c}\sum_c \left|\frac{y_{gc}-\hat{y}_{gc}}{y_{gc}}\right|$, where N_c = 144 is the number of microarray experiments included in the random tester dataset. Figure 4a shows the distribution of Δ_g for all genes included in the predicted *A. thaliana* transcriptional network. The distribution of errors has a median value of 3.66% and is significantly asymmetrical (skewness 1.709 ± 0.017, $P < 0.0001$), with most genes having a relatively low error but with some genes whose expression is estimated with errors > 10% and even in a few instances > 16%. How does this predictive performance compare to that obtained for other organisms, as for example *E. coli*? In a previous study, we constructed a transcriptional network containing 4345 genes and 328 TFs from *E. coli* [25] using a dataset containing 189 experimental conditions. For this network, the average error over the training set was similar (3.68%) to the values reported above but with the error distribution being even more asymmetrical (skewness 2.314 ± 0.017, P < 0.0001). The average error over the *E. coli* test set (4.80%) was larger. Figure 4b shows the distribution of Δ_g for gene-to-gene and gene-TFs interactions which is also significantly asymmetrical (skewness 1.455 ± 0.017, $P < 0.001$), although in this case the median error is reduced to 2.71% and in all cases the error was < 9%. Both distributions significantly differ in shape (Kolmogorov-Smirnov test $P < 0.001$) and location (Mann-Whitney test $P < 0.001$), with the latter being narrower and centered around a lower expression error. One may ask whether the predictability of our model was driven by TFs and not by non-TF genes. To test this possibility we proceeded as follows. First, we selected a random set of 1187 non-TFs genes and used them to construct the corresponding pseudo-transcriptional network.

Then we evaluated its performance as described above. The level of precision reached was undistinguishable from the previous one, with the distribution of relative expression error obtained fully overlapping with the one shown in Figure 4b (data not shown). Therefore, we conclude from this analysis that TFs do not have stronger predictive power than the rest of genes. This could be rationalized because, in terms of mathematical equations, genes that are coexpressed with the TFs have *a priori* equal chances to work as regulatory elements. On the other hand, we have also constructed an effective model excluding the TFs from the set of predictors and observed that the relative expression error decreased proportionally to the number of excluded TFs.

As a second step for the predictability of our test model, we have computed Pearson correlation coefficients (r) between the experimental and predicted gene expressions for all microarray experiments and we have observed that, as expected, genes having high r also have low Δ_g (Figure S6 in Additional data file 1). In addition, we noticed that the predictability of the expression of those genes with high r depends on a reduced set of TFs (see in Figure S7a in Additional data file 1 that the critical mass of points concentrates in a region with high r and low number of predictors), suggesting that a selective pressure exists to introduce indirect regulations as a way to increase robustness of genetic systems to dynamic environments. Figure S7a in Additional data file 1 also shows that the model does not tend to add large numbers of regulations as a way to minimize expression error and, by contrast, the highest density of values corresponds to a rather low number of regulations (between 0 and 30). The average incoming connectivity estimated for *E. coli* [25] and *S. cerevisiae* [2] were 1.56 and 2.26 regulators, respectively. The comparison of these figures with the data here reported suggests that r is not significantly increasing beyond a given number of regulations. Nonetheless, a few genes were predicted to have > 60 regulations. Looking just at the

20 most extremely regulated genes in Figure S7a in Additional data file 1, the results are somehow interesting: the two most extreme cases correspond, respectively, with gypsy- and copia-like retrotransposons (89 and 83 connections to TFs, respectively), nine genes are annotated as unknown proteins, two are annotated as belonging to the F-box family but without any assigned biological process, one has been assigned as a putative protein kinase, five have been loosely assigned to transcription, translation, transport and secondary metabolism, and the only one with a well defined function is the *At2g26330* locus that encodes for the *ERECTA* receptor of protein kinases involved in several developmental roles as well as in response to bacterial infections. Moreover, Figures S7b and S7c in Additional data file 1 show a histogram of r per gene over 1292 experiments in the training set and 144 conditions in the test set, respectively. The average r for the training set was 0.767 and very similar (0.759) for the test set. These values are on the same range that those reported in a study inferring the regulatory network (1934 genes; including 81 regulators) for *Halobacterium salinarum NRC-1* [26] using 266 experimental conditions for the training model and 131 extra experiments as test set. In this case $r = 0.788$ for the training set and $r = 0.807$ for the test set.

For illustrative purposes, Figure 5 shows the expression predicted for five best cases for the transcriptional network, each dot in the scatter plots representing a value obtained on a different hybridization experiment. The left column shows the prediction obtained using the whole dataset (1436 experiments) both as training and as tester sets, whereas the right column shows, for the same five genes, the correlation between the prediction obtained from the test model (inferred from the reduced training set of 1292 experiments) and the observations contained in the tester set (144 experiments). It is remarkable that the quality of the prediction does not change by using a reduced training set, in good agreement with the results reported for *E. coli*

[25]. Similarly, Figure S8 in Additional data file 1 shows the three best and worst predicted cases for the effective gene-to-gene interaction model inferred from the whole dataset. In this case, the R^2 for the poorly predicted genes widely ranged, with gene *At2g02120* (pathogenesis-related protein belonging to the defensin family) having the lowest determination coefficient observed.

Selection of optimality in changing environments

Organisms have a high capacity for adjusting their metabolism in response to environmental changes, food availability, and developmental state [35]. On the one hand, we have detected that GO pathways (Table 4) related with response to diverse environmental (e.g., defense against diverse pathogens, response to radiation, temperature, light intensity, or osmotic stress) and internal (development, secondary metabolism, porphyrin biosynthesis, etc…) stimuli consists of sets of genes with high incoming connectivity, that is, genes regulated by many different TFs. Therefore, this high degree of interconnection among different stimulus-related pathways allows the cell to rapidly adjust its homeostasis in response to changing environments. On the other hand, functional GO pathways associated to biological functions with expression unaffected by external stresses (e.g., glycerophospholipid and glycerophospholipid metabolic process, sulfur amino acid biosynthetic process, indole and derivative metabolic process, membrane lipid biosynthetic process, sulfured compounds biosynthetic, and Golgi vesicle transport (Table 4)), have low incoming connectivities. Notice that some GO pathways indirectly related with external stresses such as for instance indole derivatives, like camalexin, (involved in response to the bacterium *Pseudomonas syringae*) or lipid biosynthesis pathways (playing a role in defense) were not scored with high levels of connectivity and high number of FFLs involved in the GO pathway. Furthermore, the predicted master regulators of *A. thaliana* listed in

Table 2 belong to biological functions related to transcription and regulation of cellular metabolic processes (containing 812 TFs each) or RNA metabolic processes (536 TFs) that are stimulated by environmental and developmental stresses. After all, the regulatory network of *A. thaliana* governs the intra-cellular processes and modulates and determines the expression of the different programs encoded in the genome.

Networks can be decomposed into subnetworks which can be seen as their building blocks. These building blocks, generally known as motifs, are defined in terms of their frequency and are typically constituted by several promoter regions of genes expressing TFs which regulate each other in a number of well known patterns (e.g., bifans, forward, feedforward, or negative feedback loops) [36]. Certain regulatory network motifs have been described as conferring robustness to perturbations in individual edges, being the coherent feedforward loop (FFL) the prototypical example of such a robustness-conferring motif [37-40]. Therefore, we sought to characterize our inferred complex network in terms of the presence and abundance of regulatory networks motifs. An exhaustive list of the founded motifs, with their observed frequency and whether this frequency significantly deviates from the expected value from a random network are shown in Tables S2 to S5 in Additional file 2 for three- and four-element motifs both for transcriptional regulations as well as for gene-to-gene interactions. Some of the overrepresented motifs are shown in Figure 6. The third most abundant motif found is, precisely, the FFL (third raw in Figure 6a). Indeed, FFL is overrepresented among GO categories involved in stress response compared to non-stress response categories (Table 4; Fisher's exact test, $P < 0.001$).

Next, we sought to test whether the presence of FFL indeed contributed to increment the robustness of the gene expression of the involved genes. To do so, we have computed a score, ρ^*, quantifying the robustness of gene expression for all predicted

TF–gene interactions involving three nodes (Figure 6c). Figure 6e shows the distribution of the robustness score computed from the inferred regulatory network. Although it may not result apparent after the visual inspection of Figure 6e, the distribution is asymmetrical (skewness 1.881 ± 0.007, $P < 0.001$) and strongly leptokurtic (1294.051 ± 0.014, $P < 0.001$), suggesting that there are more data points in the tails than close to the mean. The data points in the upper tail correspond to the more robust interactions and, if coherent FFLs are involved in such type of interactions, they may be over-represented on this tail. This is, indeed, the case. If we look at the upper 1% values, 90.7% of them correspond to coherent FFL. By contrast, if we look at the 1% interactions around the mean value, only 5.7% correspond to FFL. Interestingly, 90.2% of motifs within the 1% lower tail of the distribution correspond to incoherent FFLs.

Discussion

We have discussed a reverse-engineered model of the *A. thaliana* cell's gene regulatory network aimed to future research projects focused on distinguishing, e.g., the molecular targets of a plant virus from the hundreds to thousands of additional gene products that may modify levels of gene expression as a side-effect. We have used a recent methodology to infer the global topology of transcription regulation from gene expression data to produce a kinetic model able to predict the alterations in gene expression in plants subjected to different external stimulus. Moreover, we have concluded that the *A. thaliana* inferred transcriptional network presents a hierarchical scale-free architecture where biological functions cluster in modules. We have identified biological functions which are highly controlled by predicted master regulators that could change their operating points in response to dynamic external

factors to produce a consistent and robustness response upon different stresses at the expense of decreasing the cellular replication rate. We have successfully applied the inferred model to predict the transcriptomic response of *A. thaliana* under all experimental conditions included in the whole dataset, and also applied the test model to predict the response in the reduced tester set, producing errors of 2 - 10% relative to the experimental value (averaging across all test experiments). Thus, we believe this modeling-validation approach constitutes an important step towards the understanding of the large-scale mode of organism's action to cope with a generally changing environment. The network model suggests that *A. thaliana* promoters are regulated by multiple TFs (Table 1), a feature which has been shown to be characteristic of eukaryotes gene regulation [2].

We have discussed a first gene regulatory model based on a transcriptional layer and a second model that embraces the first one by including gene-to-gene interactions that provides an even more accurate prediction of gene expression. Future works would consider just interactions between tissue-specific genes. Next, we have also quantified the presence of network motifs and found that FFL are overwhelmingly common, thus supporting the above notion that robustness against perturbation has been a major driving force during the evolution of plant lineages. Furthermore, we have confirmed that coherent FFL are overwhelmingly over-represented among interactions that are robust against the knock-out of the regulatory TF (Figure 6e), while incoherent FFL are so among the most sensitive interactions. Figure 6c illustrates a possible mechanism by which FFL would confer robustness. Imagine that the B product is relevant for cell survival. At the one side, deriving regulation flow throughout C is costly because it implies producing a redundant element. However, if perturbations disrupt the direct edge between A and B, the existence of C still allows the cell to obtain the precious B

without incurring into a major penalty (Figure 6d). Whether a given regulatory network may be selected to contain this sort of regulatory elements depends on the balance between the fitness costs and benefits associated with redundancy [41,42]. The fact that *A. thaliana* network topology seems to be rich in these transcriptional regulatory elements suggests that it has been evolutionary optimized to allow rapid responses to changes in the external conditions while maintaining cellular homeostasis, and hence maximizing fitness.

The reconstruction of genome-scale regulatory models constitutes a major step towards the understanding of the cellular behavior, but it also is for Synthetic Biology, where predictive models can be applied to engineer synthetic systems for biotechnological applications. Hence, *InferGene* [25] provides a mechanism to predict the changes in the biological processes when perturbing the cell in order to identify the effects of drugs, virus infection and herbicides action in plant interactomes. It may facilitate optimization of cellular processes for biotechnology applications that utilize the complex regulatory properties of genetic networks.

Conclusions

In this study, we have shown that *A. thaliana* regulatory network is scale free and clustered both characteristic properties of hierarchical networks. We also used our model to analyze the robustness in expression levels conferred by network motifs such as the coherent feedforward loop. Hence, the meta-analysis presented here has allowed us to identify regulatory and robust genetic structures. These results suggest that *A. thaliana* has evolved a high connectivity in terms of transcriptional regulations among cellular functions involved in response and adaptation to changing environments; while gene networks constitutively expressed or less related to stress

response are characterized by a lower connectivity. We successfully applied our quantitative network model to predict the full transcriptome of the plant for a set of microarray experiments, and the quality prediction evaluated by several methods.

Materials and methods

Mathematical model

Gene regulations were described by a linear model based on differential equations for the dynamics of each mRNA. Data were normalized and represented in $\log_2$ scale. Thus, the mRNA dynamics from the i^{th} gene, y_i, is given by $dy_i/dt = \alpha_i + \sum_j \beta_{ij} y_j - \delta_i y_i$, where α_i is its constitutive transcription rate, β_{ij} the regulatory effect that gene j has on gene i and δ_i the degradation coefficient. If j has no effect on the expression of i, then $\beta_{ij} = 0$. No cooperation between genes for regulation has been assumed. Time was conveniently scaled such that $\delta_i = 1$ and the model is assumed in steady-state ($y_i = \alpha_i + \sum_j \beta_{ij} y_j$), since fitting the appropriate mRNA degradation constant would require of time series data [43].

Microarray data

Steady-state mRNA expression profiles derived from transcriptional perturbations collected in the TAIR website [44] have been used in this study. We found 1187 TFs by looking for the motif "transcription factor" in the functionally annotated *A. thaliana* genome from TAIR (version 7). The dataset contains pre-processed expression data from 1436 hybridization experiments using the 22,810 probe sets spotted on Affymetrix's GeneChip *Arabidopsis* ATH1 Genome Array [45]. For this study, we consider 22,094 genes. The arrays were obtained from *NASCArrays* [46] and

AtGenExpress [47]. Data were normalized using the robust multi-array average method [27].

Inference procedure

The inference procedure consisted of two nested steps. In the first step, the global network connectivity was inferred using the *InferGene* algorithm [25]. This method uses mutual information (MI) with a local significance (*z*-score computation) to obtain the genome regulations [15]. Hence, its potential interaction between a regulator and a gene is *z*-scored, constituting an estimator of the likelihood of MI. This approach allows eliminating some false correlations and indirect influences [15]. Subsequently, we selected a *z*-score threshold for cut-off. In a second step, multiple regressions were obtained to estimate the kinetic parameters of an ODE-based regulatory model. Multilayer model were constructed to account for different types of regulations between genes and TFs. We have constructed two different models, one for transcription regulations and another to account for effective (transcription and non-transcription) regulations. In case of non-transcriptional interactions, Lasso's method was used to avoid over-fitting [48] and the effective interactions between genes giving the non-transcriptional layer were unveiled. For that end, we applied a simple and efficient algorithm based on the Gauss-Seidel method [49] that reduces the number of regulators that exceeded the *z*-score threshold for a given gene. Note that the Lasso method enriches in TFs among the predictors of the target for the 33.21% of non-constitutive genes of *A. thaliana* (i.e., the ratio between the number of TFs selected and the total number of predictors of a given gene above a threshold defined as 1187/22,094 = 0.0537). Finally, one SBML [50] file containing the transcriptional model and a plain text file containing the effective model were constructed and are available as supplementary files in Additional data file 3. These files can be viewed using

Cytoscape viewer for further analysis. Notice that the transcriptional model was embedded within the effective one. Networks are constructed by placing genes as nodes and regulations as edges. For the transcriptional model, edges only go from TFs to genes (including other TFs). For the non-transcriptional model, edges connect two genes, the regulator and the target and, thus, the resulting network is directional.

Model validation

The performance of the inferred model topology was evaluated using a reference network defined by taking those genes with known transcriptional regulation. For that, the *AtRegNet* platform [51] linking *cis*-regulatory elements and TFs into regulatory networks was used. Only those interactions among genes included in that reference set were evaluated. The fraction of interactions that were correctly predicted by the model (precision, *P*) and the fraction of all known interactions that were discovered by the model (sensitivity, *S*) were used to compute a performance statistic defined as $F = 2PS/(P+S)$ [16]. We have to notice that the number of transcriptional regulations experimentally confirmed and compiled in *AtRegNet* is quite limited, containing only 448 reported interactions between TFs and genes. Therefore it is difficult to obtain an accurate value for the performance of the model.

To validate the predictive power of the methodology, we constructed two transcription models. The first one was obtained by using the 1436 microarrays for training. For the second model (test model), of all these microarrays, 1292 were used as training set (90%) whereas 144 randomly chosen ones (10%) were retained for validation studies.

Motif detection and analysis

The FANDOM program [52] has been used to detect motifs of 3 and 4 genes in the predicted *A. thaliana* regulatory model. Those motifs statistically significant have *z*-scores > 2.

The robustness of gene expression to perturbations in the underlying motifs was evaluated for each interaction as follows. In a scheme as the one illustrated in Figure 6c, TF *A* operates on gene *B* but also may act upon a second transcription factor *C* which, itself, may also interact with the promoter region of *B* activating its expression. For such a system, we define the robustness score $\rho_{AB} = (y_B^+ - y_B^-)/\beta_{AB} y_A$ to quantify the impact that removing TF *A* has in the expression of gene *B*; where y_B^+ represents the measured expression of gene *B* when the *A* exists and y_B^- after it has been removed. The difference in gene expression is normalized by the expression level of the transcription factor *A*, y_A, and the strength of its regulation, β_{AB}, on the expression of *B*. If *A* is removed ($y_A \to 0$) and no alternative pathway exist, then $\rho_{AB} \to 1$. However, if *C* exists, as it is the case for the FFL, then $\rho_{AB} \neq 1$, with its sign being determined by $y_B^+ - y_B^-$ and the sign of β_{AB}. This score is unbounded, thus for convenience we further normalized it as $\rho_{AB}^* = (\rho_{AB} - 1)/\max_{\forall i,j}(\rho_{ij})$, which is now contained in the interval [–1, 1]. Values of ρ_{AB}^* close to 1 would correspond to maximally robust motifs, whereas values close to zero correspond to motifs not contributing to the robustness of the network. Values close to –1 correspond to incoherent motifs, that is, gene circuits implementing antagonistic regulations [34].

Abbreviations

F (absolute efficiency); FFL (feed-forward loop); *FN* (false negative); *FP* (false positive); MI (mutual information); *P* (precision); *S* (sensitivity); TFs (transcription factors); *TP* (true positives).

Authors' contributions

SFE conceived the study. JC, GR and AJ performed all the computations. All authors analyzed the data and contributed to writing the manuscript.

Additional data files

The following additional data are available with the online version of this paper. Additional data file 1 contains the eight supplementary figures mentioned in the text. Additional data file 2 contains the five supplementary tables mentioned in the text. Additional data file 3 contains the effective and transcriptional models.

Acknowledgements

We thank J. Forment for help with computer resources and M. A. Blázquez for critical reading of the manuscript and useful suggestions. This work was supported by grants BFU2006-14819-C02-01/BMC and TIN2006-12860 from the Spanish Ministerio de Ciencia e Innovación to S.F.E and A.J., respectively; FP6-NESTs 043340 (BioModularH2) and 043338 (Emergence), FP7-KBBE-212894 (Tarpol), the Structural Funds of the European Regional Development Fund (ERDF), the 91-A3405-ATIGE Genopole/UEVE and the MIT-France grants to A.J. J.C, G.R. and A.J. acknowledge the HPC-Europa program (RII3-CT-2003-506079). G.R. was supported by a graduate fellowship from the Generalitat Valenciana and an EMBO Short-term fellowship (ref. ASTF-343.00-2007). S.F.E. also acknowledges support from the Santa Fe Institute.

References

1. Gutiérrez-Ríos RM, Rosenblueth DA, Loza JA, Huerta AM, Glasner JD, Blattner FR, Collado-Vives J: **Regulatory network of *Escherichia coli*: consistency between literature knowledge and microarray profiles.** *Genome Res* 2003, **13:**2435-2443.
2. Lee TI, Rinaldi NJ, Robert F, Odom DT, Bar-Joseph Z, Gerber GK, Hannett NM, Harbison CT, Thompson CM, Simon I, Zeitlinger J, Jennings EG, Murray HL, Gordon DB, Ren B, Wyrick JJ, Tagne JB, Volkert TL, Fraenkel E, Gifford DK: **Transcriptional regulatory networks in *Saccharomyces cerevisiae*.** *Science* 2002, **298:**799-804.
3. Kim SK, Lund J, Kiraly M, Duke K, Jiang M, Stuart JM, Eizinger A, Wylie BN, Davidson GS: **A gene expression map for *Caenorhabditis elegans*.** *Science* 2001, **293:**2087-2092.
4. Ma S, Gong Q, Bohnert HJ: **An *Arabidopsis* gene network based on the graphical Gaussian model.** *Genome Res* 2007, **17:**1614-1625.
5. Mentzen WI, Wurtele ES: **Regulon optimization in *Arabidopsis*.** *BMC Plant Biol* 2008, **8**:99.
6. Lee HK, Hsu AK, Sajdak J, Qin J, Pavlidis P: **Coexpression analysis of human genes across many microarray data sets.** *Genome Res* 2004, **14:**1085-1094.
7. Eisen M, Spellman P, Brown P, Botstein D: **Cluster analysis and display of genome-wide expression patterns.** *Proc Natl Acad Sci USA* 1998, **95**:14863-14868.
8. Alon U, Barkai N, Notterman D, Gish K, Ybarra S, Mack D, Levine A: **Broad patterns of gene expression revealed by clustering analysis of tumor and normal colon tissues probed by oligonucleotide arrays.** *Proc Natl Acad Sci USA* 1999, **96**:6745–6750.

9. Ben-Dor A, Shamir R, Yakhini Z: **Clustering gene expression patterns.** *J Comput Biol* 1999, **6**:281–297.

10. Dhaeseleer P, Liang S, Somogyi R: **Genetic network inference: from co-expression clustering to reverse engineering.** *Bioinformatics* 2000, **16**:707-726.

11. Ihmels J, Friedlander G, Bergmann S, Sarig O, Ziv Y, Barkai N: **Revealing modular organization in the yeast transcriptional network.** *Nat Genetics* 2002, **31**:370–377.

12. Butte A, Kohane I: **Mutual information relevance networks: functional genomic clustering using pairwise entropy measurements** *Pacific Symp Biocomput* 2000, **5:**415–426.

13. Basso K, Margolin AA, Stolovitzky G, Klein U, Dalla-Favera R, Califano A: **Reverse engineering of regulatory networks in human B cells.** *Nat Genetics* 2005, **37:**382–390.

14. Margollin A, Nemenman I, Basso K, Wiggins C, Stolovitzky G, dellaFavera R, Califano A: **ARACNE: an algorithm for the reconstruction of gene regulatory networks in a mammalian cellular context.** *BMC Bioinformatics* 2006, **7:**S7.

15. Faith JJ, Hayete B, Thaden JT, Mogno I, Wierzbowski J, Cottarel G, Kasif S, Collins JJ, Gardner TS: **Large-scale mapping and validation of *Escherichia coli* transcriptional regulation from a compendium of expression profiles.** *PLoS Biol* 2007, **5:**e8.

16. Meyer PE, Kontos K, Lafitte F, Bontempi G: **Information-theoretic inference of large transcriptional regulatory networks.** *EURASIP J Bioinf Syst Biol* 2007, **2007**:79879.

17. Husmeier D: **Sensitivity and specificity of inferring genetic regulatory interactions from microarray experiments with dynamic bayesian networks.** *Bioinformatics* 2003, **19:**2271–2282.

18. Yu J, Smith V, Wang P, Hartemink A, Jarvis E: **Advances to bayesian network inference for generating causal networks from observational biological data.** *Bioinformatics* 2004, **20:**3594-3603.

19. Fujita A, Sato JR, Garay-Malpartida HM, Yamaguchi R, Miyano S, Sogayar MC, Ferreira CE: **Modeling gene expression regulatory networks with the sparse vector autoregressive model.** *BMC Syst Biol* 2007, **1**:39.

20. Steinke F, Seeger M, Tsuda K: **Experimental design for efficient identification of gene regulatory networks using sparse bayesian models.** *BMC Syst Biol* 2007, **1**: 51.

21. Ma S, Bohnert HJ: **Integration of *Arabidopsis thaliana* stress-related transcript profiles, promoter structures, and cell-specific expression.** *Genome Biol* 2007, **8:**R49.

22. Gardner T, diBernardo D, Lorenz D, Collins JJ: **Inferring genetic networks and identifying compound mode of action via expression profiling.** *Science* 2003, **301**:102–105.

23. Di Bernardo D, Thompson M, Gardner T, Chobot S, Eastwood E, Wojtovich A, Elliott S, Schaus S, Collins JJ: **Chemogenomic profiling on a genome-wide scale using reverse-engineered gene networks.** *Nat Biotechnol* 2005, **3**:377–383.

24. Bonneau R, Reiss D, Shannon P, Facciotti M, Hood L, Baliga N, Thorsson V: **The inferelator: an algorithm for learning parsimonious regulatory networks from systems-biology data sets de novo.** *Genome Biol* 2006, **7**:R36.

25. Carrera J, Rodrigo G, Jaramillo A: **Model-based redesign of global transcription regulation.** *Nucl Acids Res* 2009, **37**:e38.

26. Bonneau R: **A predictive model for transcriptional control of physiology in a free living cell.** *Cell* 2007, **131**:1354-1365.

27. Irizarray RA, Hobbs B, Collin F, Beazer-Barclay YD, Antonellis KJ, Scherf U, Speed TP: **Exploration, normalization, and summaries of high density oligonucleotide array probe level data.** *Biostatistics* 2003, **4:**249-264.

28. Shannon P, Markiel A, Ozier O, Baliga N, Wang J, Ramage D, Amin N, Schwikowski B, Ideker T: **Cytoscape: a software environment for integrated models of biomolecular interaction networks.** *Genome Res* 2003, **13:**2498–504.

29. Albert R, Barabási AL: **Statistical mechanics of complex networks**. *Rev Mod Phys* 2002, **74**:47-97.

30. Albert R: **Scale-free networks in cell biology**. *J Cell Sci* 2005, **118**: 4947-4957.

31. Barabási AL, Oltvai ZN: **Network biology: understanding the cell's functional organization.** *Nat Rev Genet* 2004, **5**:101-113.

32. Khanin R, Wit E: **How scale-free are biological networks**. *J Comp Biol* 2006, **13**: 810-818.

33. Ravasz E, Barabási AL: **Hierarchical organization of complex networks**. *Phys Rev E* 2003, **67**: 026112.

34. Ravasz E, Somera AL, Mongru DA, Oltvai ZN, Barabási AL: **Hierarchical organization of modulatiry in metabolic networks**. *Science* 2002, 297:1551-1555.

35. Oltvai ZN, Barabási AL: **Life's complexity pyramid.** *Science* 2002, **298:**763-764.

36. Kashtan N, Itzkovitz S, Milo R, Alon U: **Topological generalizations of network motifs.** *Phys Rev E* 2004, **70:**031909.

37. Mangan S, Alon U: **Structure and function of the feed-forward loop network motif.** *Proc Natl Acad Sci USA* 2003, **100**:11980-11985.

38. Mangan S, Zalsaver A, Alon U: **The coherent feedforward loop serves as a sign-sensitive delay element in transcription networks.** *J Mol Biol* 2003, **334**:197-204.

39. Hayot F, Jayaprakash C: **A feedfoward loop motif in transcriptional regulation: induction and repression.** *J Theor Biol* 2005, **234**:133-143.

40. Alon U: **Network motifs: theory and experimental approaches.** *Nat Rev Genet* 2007, **8**:450-461.

41. Sanjuán R, Elena SF: **Epistasis correlates to genomic complexity.** *Proc Natl Acad Sci USA* 2006, **103:**14402-14405.

42. Dekel E, Alon U: **Optimality and evolutionary tuning of the expression level of a protein.** *Nature* 2005, **436:**588-592.

43. Bar-Joseph Z: **Analyzing time series gene expression data.** *Bioinformatics* 2004, **20:**2493-2503.

44. TAIR [www.arabidopsis.org].

45. ATH1 Genome array [http://www.affymetrix.com/products_services/arrays/specific/arab.affx].

46. *NASCArrays* [http://affymetrix.arabidopsis.info/narrays/experimentbrowe.pl].

47. *AtGenExpress* [http://www.arabiodpsis.org/info/expression/ATGenExpress.jsp].

48. Tibshirani R: **Regression shrinkage and selection via de Lasso.** *J R Statist* 1996, **58:**267-288.

49. Shevade SK, Keerthi SS: **A simple and efficient algorithm for gene selection using sparse logistic regression**. *Bioinformatics* 2003, **19**:2246-2253.

50. Hucka M, Bolouri H, Finney A, Sauro HM, Doyle JC, Kitano H, Arkin AP, Bornstein BJ, Bray D, Cornish-Bowden A, Cuellar AA, Dronov S, Gilles ED, Ginkel M, Gor V, Goryanin II, Hedley WJ, Hodgman TC, Hofmeyr JH, Hunter PJ, Juty NS, Kasberger NS, Kremling S, Kummer U, Novère NL, Loew LM, Lucio D, Mendes P, Minch E, Mjolsness ED *et al*: **The systems biology markup language (SBML): A medium for representation and exchange of biochemical network models.** *Bioinformatics* 2003, **19**:524–531.

51. *AtRegNet* [http://arabidopsis.med.ohio-state.edu/RGNet].

52. Wernicke S, Rasche F: **FANMOD: a tool for fast network motif detection.** *Bioinformatics* 2006, **22:**1152-1153.

Figure 1. Plot of the inferred regulatory network of *A. thaliana* visualized using Cytoscape. Nodes only represent TFs.

Figure 2. Analyses of the regulatory network of *A. thaliana*. Distributions for the transcriptional network of (a) outcoming connectivity showing the master regulators from the Table 2 in a different color, (b) incoming connectivity, (c) clustering coefficient, and (d) betweenness centrality. Distributions for the non-transcriptional network of (e) outcoming connectivity and (f) incoming connectivity.

Figure 3. Transcriptional subnetworks with high clustering coefficients corresponding to the following GO pathways: (a) auxin metabolic process, (b) response to other organism, (c) response to heat, (d) systemic acquired resistance (experimentally verified regulations are represented with thick edges), (e) response to salt stress, and (f) immune response.

Figure 4. Histogram of the relative gene expression error in (a) the transcriptional test model (with an average error of 0.0402) and in (b) the effective model (with an average error of 0.0280). Errors were obtained from the comparison of the predicted model obtained from the training dataset and the experimental determinations contained in the random tester dataset.

Figure 5. Predictive power on gene expression of the transcriptional model of *A. thaliana* inferred from the whole data set (1436 conditions) and the test model from 1292 microarray experiments, used as training set. The left column shows the regression coefficient (R^2) between the model and experimental profiles across the whole data set for the five best predicted genes. The right column shows R^2 between

the test model and the 144 experimental profiles used as tester set for the same five genes. In either case, correlation coefficients were highly significant.

Figure 6. Network motifs of three (a) and four (b) genes found in the transcriptional network of *A. thaliana*. Here we plot the most statistically significant ones (see the Supplementary Materials for a complete list of motifs). We show a motif significantly overrepresented, feed-forward loop (c), where an external factor could inhibit the regulation of the gene A to the gene B, but this structure provides an indirect regulation by means of the gene C. On other hand, we show in (d) the evolution of the qualitative development of a plant with motifs (dashed line) and without motifs (solid line) under changing environments. We note that it exists an evolutionary optimization to include topologic units such as feed-forward loop providing robustness under external factors despite decreasing system's fitness (see area I and II) due to an exceed of gene expression of those genes providing indirect interactions. Panel (e) shows the distribution of normalized robustness coefficients (ρ^*) computed for all interactions between TFs and genes.

Table 1

Topological parameters of the inferred transcription network of *A. thaliana*

Parameter	**Value**
Clustering coefficient	0.319
Network diameter	13
Characteristic path length	5.065
Number of connected genes	18,169
Number of regulations inferred	128,422
Network density	7.78×10^{-4}
Constitutive genes	3952 (17.89%)
Genes regulated by one TF	3111 (14.08%)
Genes regulated by two TFs	2352 (10.64%)
Genes regulated by three TFs	1966 (8.90%)
Genes regulated by four TFs	1606 (7.27%)
Genes regulated by five TFs	1393 (6.30%)
Genes regulated by more than five TFs	7714 (34.91%)

Table 2

Top 10 of the TFs with more regulatory effects (i.e., highest outcoming connectivity)

Transcription Factor	**Outcoming Connectivity**	**Gene Annotation**	**GO pathways (level 5)**
At4g17695	1254	KAN3 (KANDI 3)	Transcription; regulation of cellular metabolic process
At1g77200	1103	AP2	Transcription; regulation of cellular metabolic process; RNA metabolic process
At2g17040	1100	ANAC036 (*Arabidopsis* NAC domain containing protein 36)	Transcription; regulation of cellular metabolic process; RNA metabolic process
At5g16560	1100	KAN	Reproductive structure development; regionalization; organ development; cell fate commitment
At2g47900	971	AtTLP3 (tubby like protein 3)	Transcription; regulation of cellular metabolic process
At2g28700	921	AGL46	Transcription; regulation of cellular metabolic process; RNA metabolic process
At5g07690	850	MYB29 (myb domain protein 29)	Transcription; response to gibberellin stimulus; regulation of cellular metabolic process; RNA metabolic process
At4g14920	846	PHD finger	Transcription; regulation of cellular metabolic process; RNA metabolic process
At3g23240	816	ATERF1/ERF1 (ethylene response factor 1)	Response to ethylene stimulus; transcription; regulation of cellular metabolic process; intracellular signaling cascade; two-component signal transduction system; RNA metabolic process
At3g30210	721	MYB121 (myb domain protein 121)	Response to abscisic acid stimulus; transcription; regulation of cellular metabolic process; RNA metabolic process

Table 3

Clustering coefficient of different GO pathways in *A. thaliana*

GO pathways	Clustering coefficient*	# connected genes	# genes
Auxin metabolic process	0.643	7	31
Response to heat	0.455	44	93
Hydrogen transport	0.335	20	54
Gravitropism	0.250	8	24
Alcohol biosynthetic process	0.233	5	18
Response to salt stress	0.204	87	148
Systemic Acquired Resistance	0.201	12	21
Immune response	0.190	55	112
Cell morphogenesis	0.153	72	156
Response to other organism	0.105	92	147
Response to bacterium	0.099	34	87
Response to light stimulus	0.088	138	246

*The clustering coefficient for random subnetworks is 0.005, as computed from 10 subsets of 100 genes each.

Table 4

Average incoming connectivity for the GO pathways from all levels in *A. thaliana*

GO pathways*	**# genes**	**# TFs†**	**# TF/# genes$**	**# FFLs‡**
Top 5 with the highest total number of TFs				
Response to other organisms	296	2249	7.6	9865
Secondary metabolic process	284	1964	6.9	3321
Response to temperature stimulus	238	1650	6.9	10151
Anatomical structure morphogenesis	291	1537	5.3	13275
Response to radiation	250	1524	6.1	6233
Top 5 with the lowest total number of TFs				
Glycerophospholipid metabolic process	21	38	1.8	69
Sulfur amino acid biosynthetic process	24	60	2.5	13
Gametophyte development	24	62	2.6	1
Cellular morphogenesis in differentiation	25	68	2.7	78
Indole and derivative metabolic process	22	71	3.2	46
Top 5 with the highest relative number of TFs				
Defense response to fungus	26	355	13.7	4353
Photosynthesis	80	1064	13.3	2459
Response to light intensity	26	334	12.8	2652
Chlorophyll biosynthetic process	22	243	11.0	443
Porphyrin biosynthetic process	39	421	10.8	754
Top 5 with the lowest relative number of TFs				
Glycerophospolipic metabolic process	21	38	1.8	0
Membrane lipid biosynthetic process	48	111	2.3	121
Sulfur compound biosynthetic process	32	75	2.3	98

Golgi vesicle transport	44	104	2.4	47
Biogenic amine metabolic process	32	76	2.4	53

*Only GO pathways with a number of involved genes larger than 20 and lower than 300 from all levels were selected.

†Total number of TFs that regulate the genes of the GO pathway.

$Relative number of TFs.

‡Total number of feed-forward loops involved in the GO pathway.

Additional data file 1 (pdf file) contains:

- **Supplementary Figure 1.** *Z*-score distribution from the mutual information calculation between all pairs of gene-transcription factor.
- **Supplementary Figure 2.** Number of regulations of model depending on the cut-off threshold selection.
- **Supplementary Figure 3.** Efficiency (precision, sensitivity and *F*-score) of the transcriptional model with respect to the reference set. The vertical dashed line indicates the optimum value for the *z* threshold (= 5) according to the *F* value.
- **Supplementary Figure 4.** Gene distribution in the pathways (clusters) found in the transcriptional network.
- **Supplementary Figure 5.** Stress distribution of the transcriptional network.
- **Supplementary Figure 6.** Absolute and relative gene expression errors versus the regression coefficient between the experimental and predicted gene expressions for all conditions from the training set.
- **Supplementary Figure 7.** Regression coefficient between the experimental and predicted gene expressions for all conditions versus the number of TFs regulating that gene.
- **Supplementary Figure 8.** Predictive power on gene expression of the effective model (including the transcriptional and non-transcriptional layers). We show the regression coefficient (R^2) between the model and experimental profiles across the 1436 conditions for the best (top) and worst (bottom) predicted genes.

Additional data file 2 (pdf file) contains:

- **Supplementary Table 1.** Fit of the distributions of outcoming and incoming connectivities for the transcriptional and non-transcriptional models to different statistical distributions.
- **Supplementary Table 2.** Three-gene motifs for the transcriptional model showing the abundance and the statistical significance.
- **Supplementary Table 3.** Four-gene motifs for the transcriptional model showing the abundance and the statistical significance.
- **Supplementary Table 4.** Three-gene motifs for the non-transcriptional model showing the abundance and the statistical significance.
- **Supplementary Table 5.** Four-gene motifs for the non-transcriptional model showing the abundance and the statistical significance.

Additional data file 3 (zip file) contains:

- **Effective model.** Text file.
- **Transcriptional model.** SBML file.

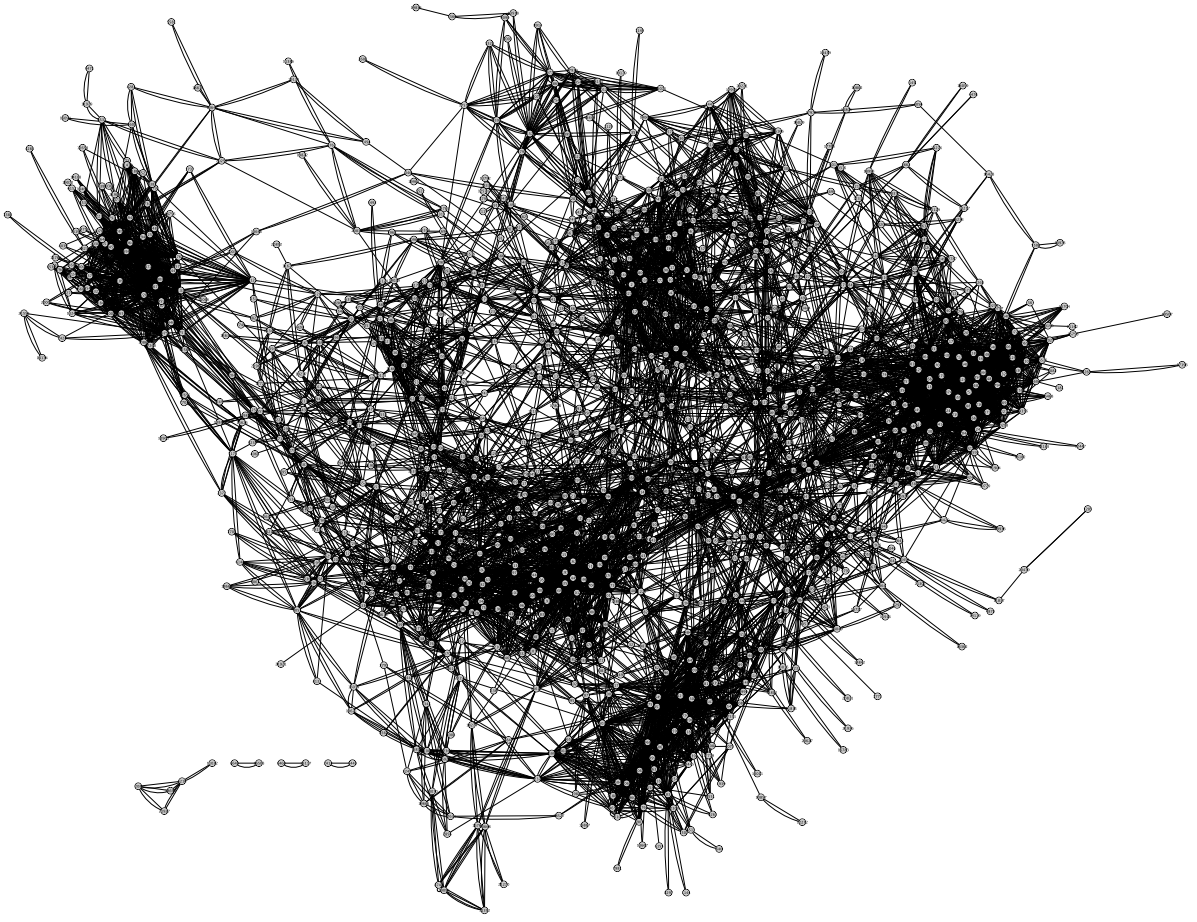

Figure 1

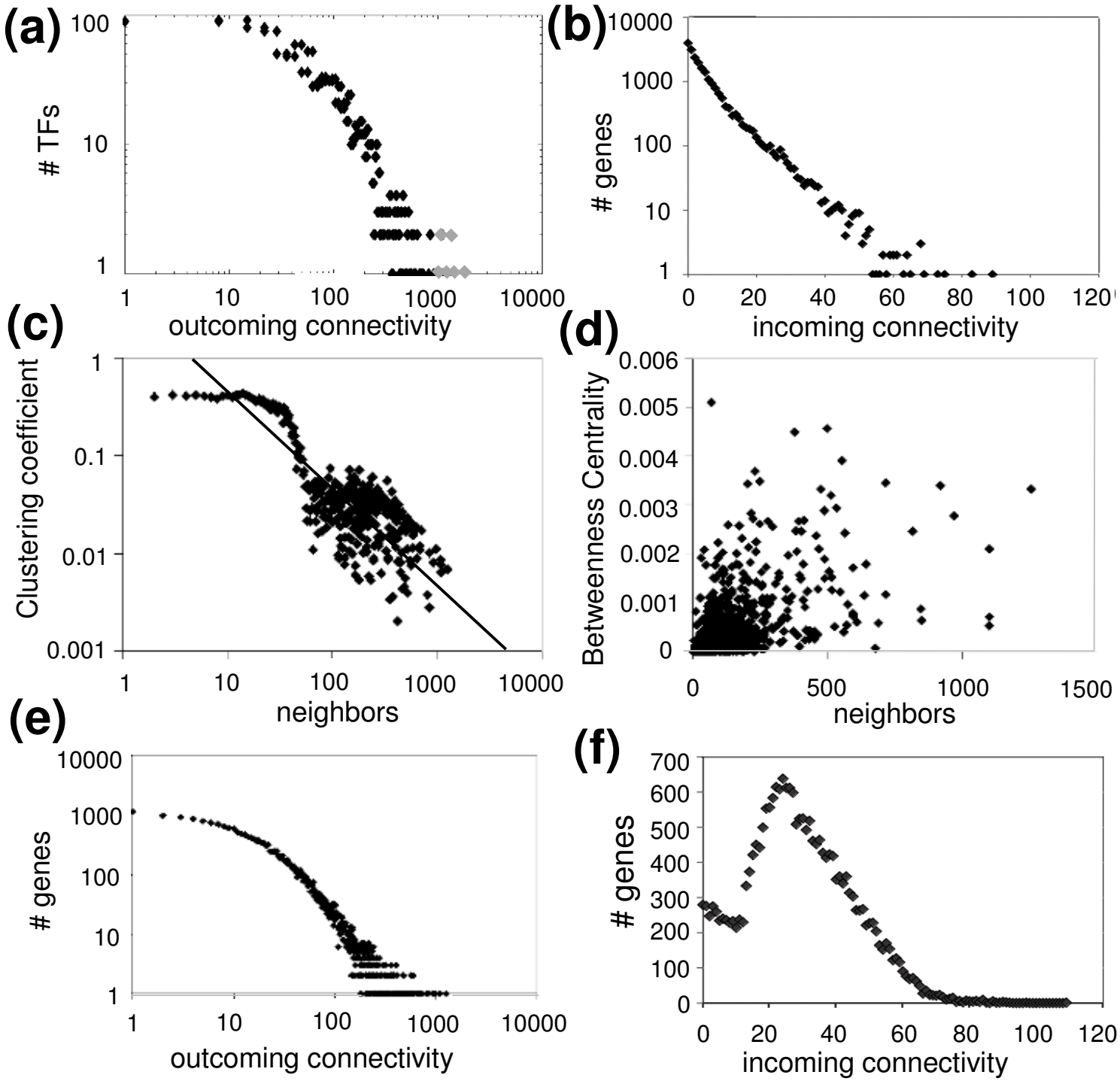
(a)
TFs
outcoming connectivity
(b)
genes
incoming connectivity
(c)
Clustering coefficient
neighbors
(d)
Betweenness Centrality
neighbors
(e)
genes
outcoming connectivity
(f)
genes
incoming connectivity

Figure 2

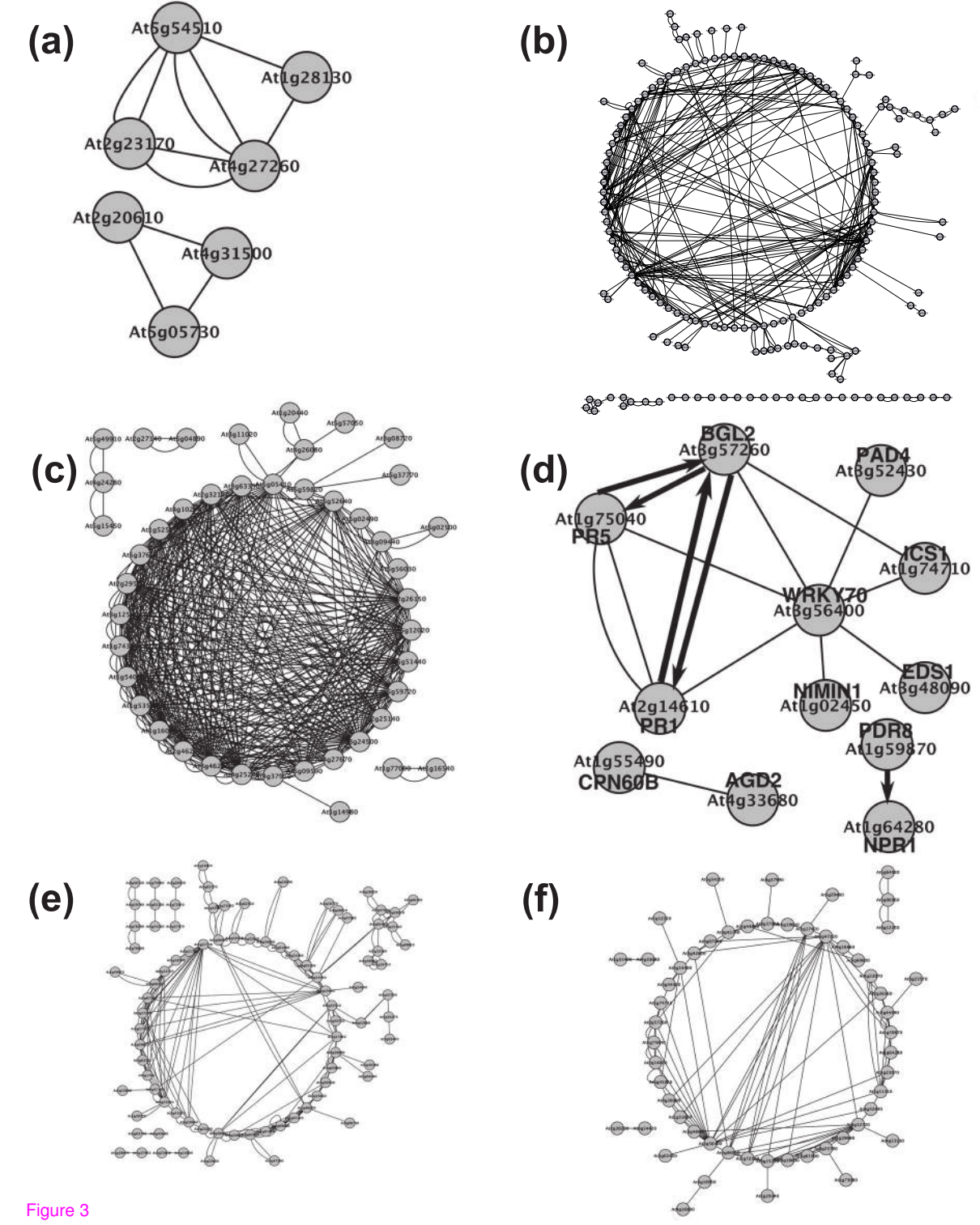
(a)
At5g54510
At1g28130
At2g23170
At4g27260
At2g20610
At4g31500
At5g05730
(b)
(c)
(d)
BGL2
At3g57260
PAD4
At3g52430
At1g75040
PR5
ICS1
At1g74710
WRKY70
At3g56400
EDS1
At3g48090
NIMIN1
At1g02450
At2g14610
PR1
PDR8
At1g59870
At1g55490
CRN60B
AGD2
At4g33680
At1g64280
NPR1
(e)
(f)

Figure 3

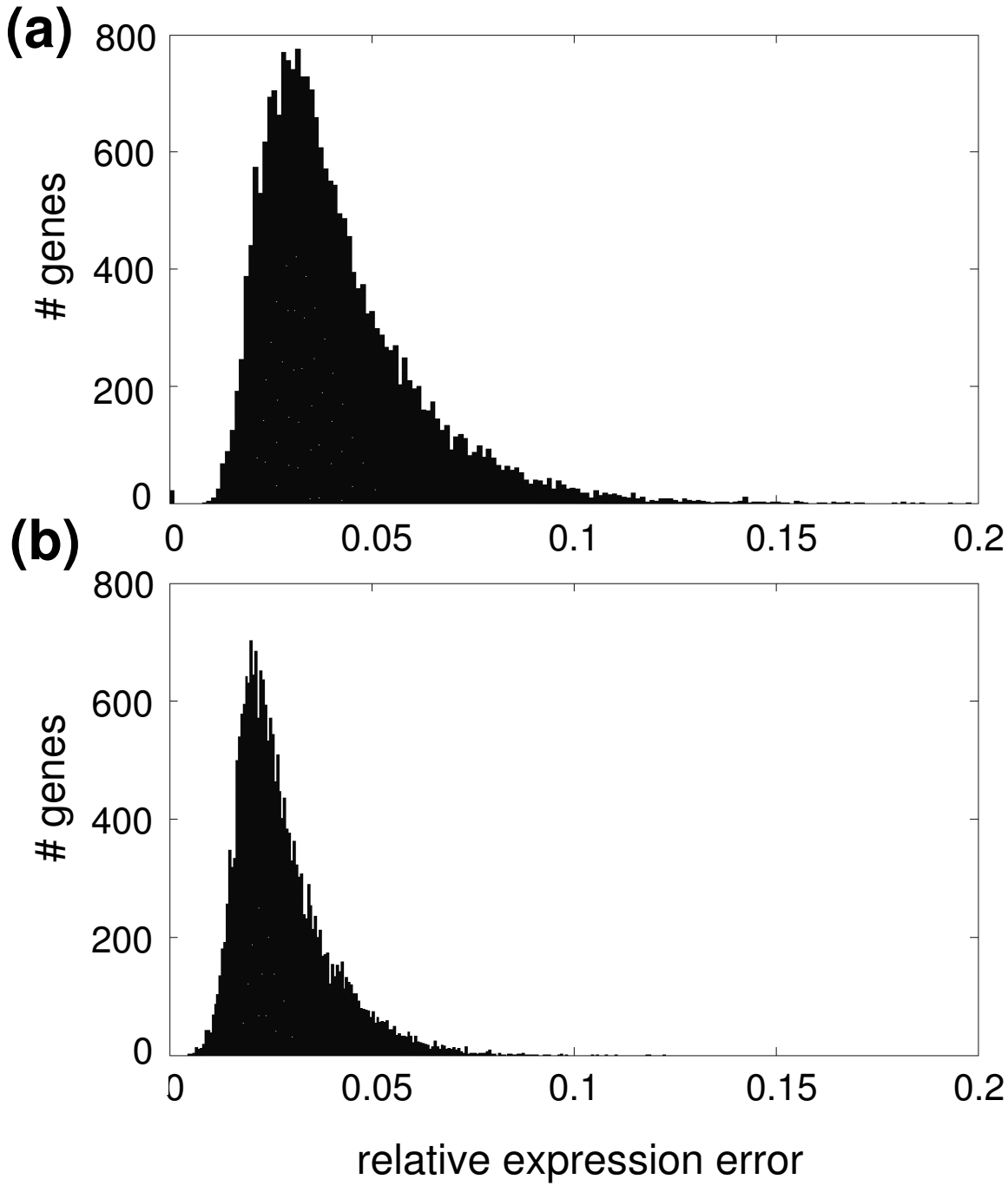
(a)
800
600
400
200
0
genes
0
0.05
0.1
0.15
0.2
(b)
800
600
400
200
0
genes
0
0.05
0.1
0.15
0.2
relative expression error

Figure 4

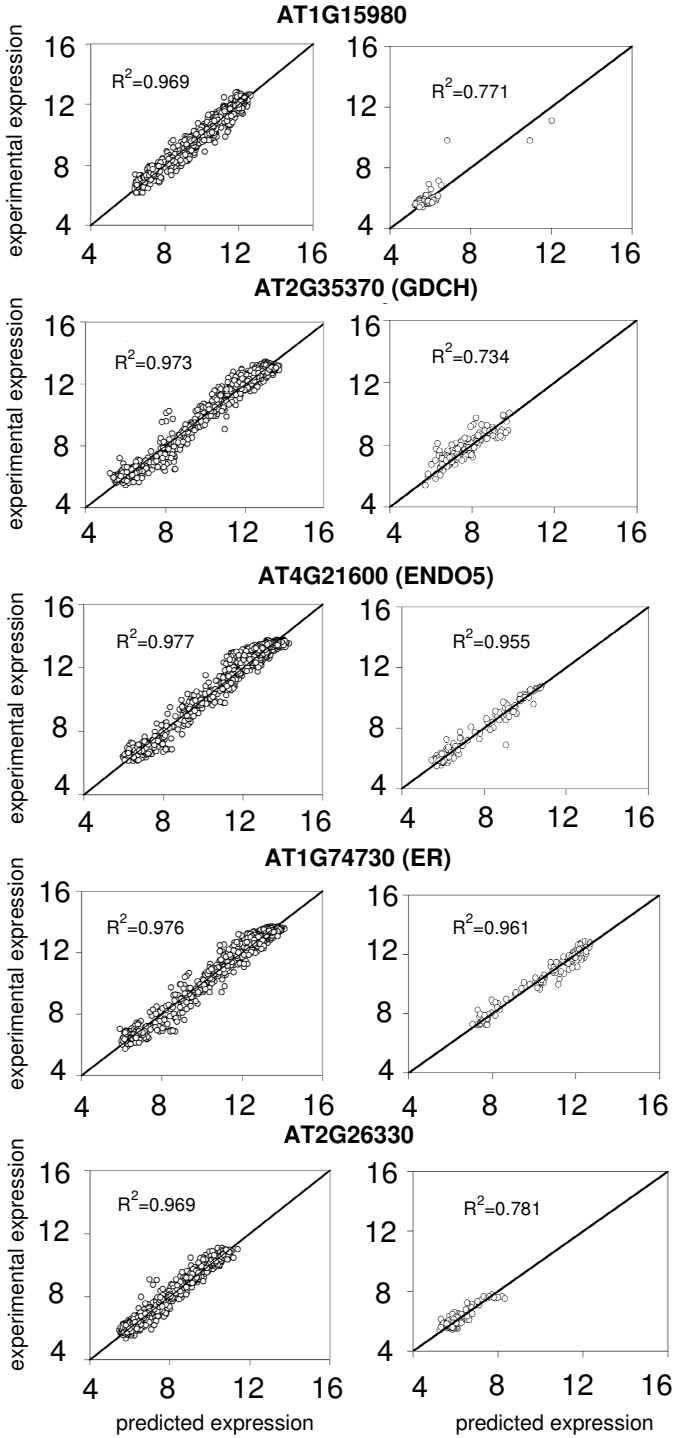
AT1G15980
R2=0.969
R2=0.771
AT2G35370 (GDCH)
R2=0.973
R2=0.734
AT4G21600 (ENDO5)
R2=0.977
R2=0.955
AT1G74730 (ER)
R2=0.976
R2=0.961
AT2G26330
R2=0.969
R2=0.781
experimental expression
predicted expression
predicted expression
4
8
12
16

Figure 5

(a)

Motif	Frequency (%)	Z-score
	1.485	282.83
	0.038451	197.94
	0.20052	59.349
	0.016166	48.038

(b)

Motif	Frequency (%)	Z-score
	0.02014	431.21
	0.25521	238.52
	0.001981	91.545
	0.017829	77.561

(c)

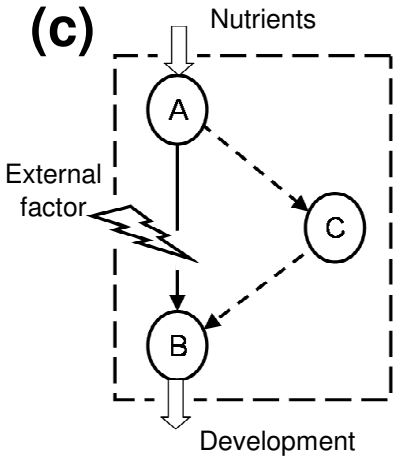

(d)

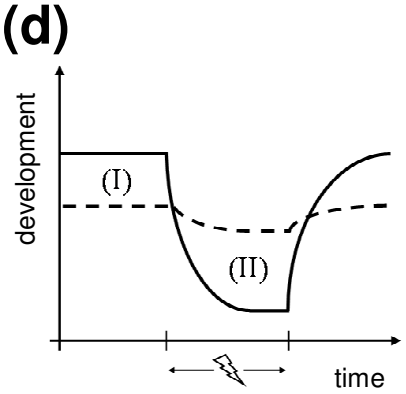

(e)

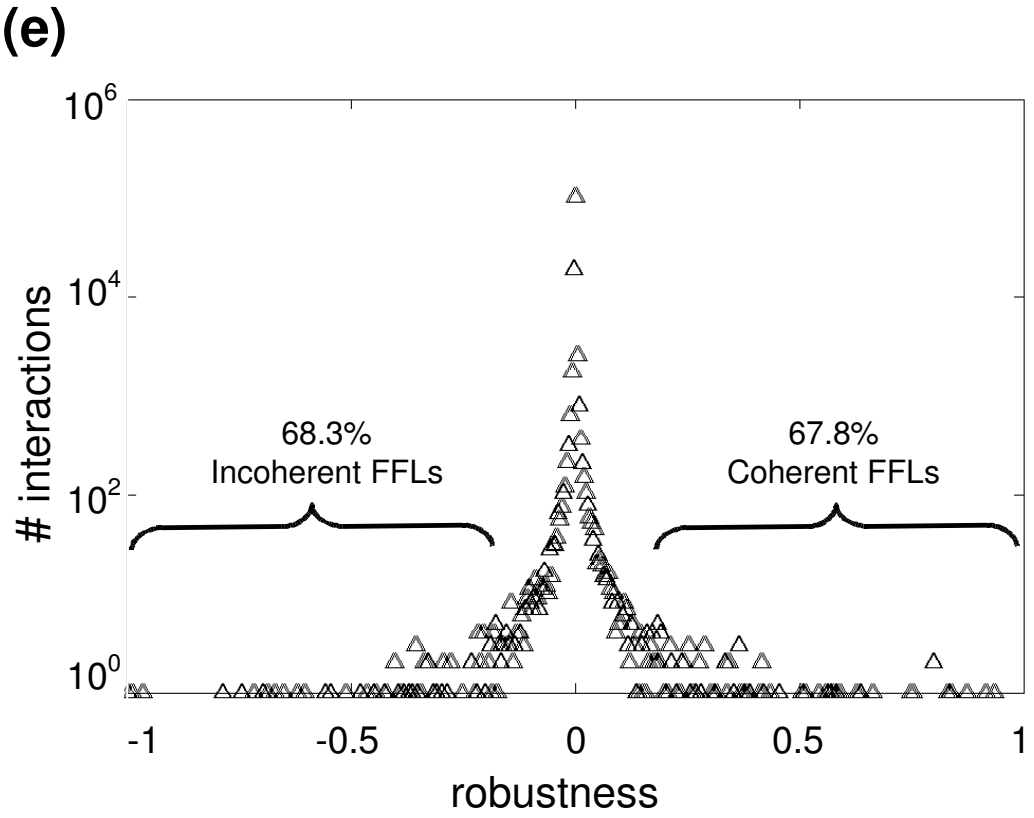

Figure 6

Additional files provided with this submission:

Additional file 1: additional data file 1.pdf, 142K
http://genomebiology.com/imedia/1619287295289252/supp1.pdf
Additional file 2: additional data file 2.pdf, 437K
http://genomebiology.com/imedia/1359557247302742/supp2.pdf
Additional file 3: additional data file 3.zip, 6122K
http://genomebiology.com/imedia/6158704633027420/supp3.zip